EUV lithography patterning using Multi-Trigger Resist

C. Popescu[a], G. O'Callaghan[a], A. McClelland[a], C. Storey[a], J. Roth[b], E. Jackson[b], A.P.G. Robinson[a,c]

[a]*Irresistible Materials, Birmingham Research Park, Birmingham, UK*
[b]*Nano-C, 33 Southwest Park, Westwood, MA, USA*
[c] *School of Chemical Engineering, University of Birmingham, B15 2TT, UK*

e-mail: a.p.g.robinson@bham.ac.uk

Keywords: EUV lithography, photoresist, molecular resist, multi-trigger resist, chemical amplification

ABSTRACT

Research and development of EUV photoresists capable of supporting future requirements such as high-NA EUV continues. It is foreseen that, to contend with much higher photon-shot noise, resists will require high EUV absorbance to offset the need for thin films in high-NA, where depth of focus may be less than 20nm. We are developing a photoresist based on the multi-trigger concept, which seeks to suppress roughness using a new photoresist mechanism, and which is based on molecular rather than polymeric materials to maximize resolution. MTR Resist absorbance of greater than 18 μm^{-1} has been measured.

Here we present recent NXE3400 results where, by modifying the PAG to optimize the reactions rates in the MTR mechanism, we have reduced the dose requirement compared to the orthodox high opacity MTR resists previously presented. Lines of 14 nm width at p28 nm can be patterned at a dose between 21 mJ/cm^2 and 48 mJ/cm^2 dependent on formulation ratio, with optimum LWR (3.9 nm, biased) occurring at 43 mJ/cm^2 with a film thickness of 20.7 nm. Similarly, we present p34 pillars patterned between 21 mJ/cm^2 and 59 mJ/cm^2 doses for 17 nm diameter pillars, with a minimum LCDU for 19 nm diameter pillars of 3.05 nm occurring with a 21.7 nm FT at 58 mJ/cm^2. The same resist can pattern p36 pillars at 52 mJ/cm^2 with an LCDU of 3.44 nm at 18 nm diameter with no measured defects between 15.9 nm and 18.1 nm diameter. The impact of the substrate (such as use of various organic underlayers or SOG layers) on defectivity issues such as bridging or falling pillars will be presented here.

1. INTRODUCTION

The search for the perfect candidate to support the next generation EUV lithography and the implementation of high-NA in industry continues. It becomes more definite that development of new photoresist mechanisms is required, and non-chemically amplified resists (non-CAR) are drawing more attention than ever before. As chemically amplified resists (CAR) are expected to reach a plateau in performance when it comes to simultaneously achieving the ultimate resolution, low line edge roughness, high sensitivity and low defectivity in high-NA, progress of non-CAR materials becomes necessary. [1–3] But there remain many unknowns which are slowing down this development, most important being the mechanism by which the EUV photons interact within the photoresist film.

The use of high energy photons in EUV lithography has shifted the photoresist chemistry towards secondary electron chemistry opening a wide space for novel resist mechanisms to be developed. However, the details of the interactions of low energy electrons with resist molecules are not entirely understood and the chemical events involved in the resist

mechanism are still being researched. [4] Various models of photo-acid generation have been proposed to explain the interactions taking place within photoresists during EUV exposures. Most studies focused on the possibility that multiple ionization events are followed by electron recombination with PAG molecules leading either directly [5] or indirectly [6] to acid generation. More recent work leaded by Brainard and co-workers, however, suggests an alternative mechanism based on internal excitations contributing to acid generation. [4,7]

Furthermore, underlayer choice can play a very important role in the overall performance of the resists. The events occurring at the interface between the photoresist and the silicon wafer are modulated by the chemical composition and therefore the chemical and physical properties of the underlayer. These events can contribute beneficially or detrimentally towards resolution and roughness in the features patterned. [8,9] Not only that, the underlayer choice also affects the metrology introducing optical contrast variations depending on the underlayer used. [10] Finally, the film thickness of the photoresist and underlayers used in high-NA tools will have to scale to accommodate the reduced depth of focus of the new tools. This will only amplify the metrology issues and increase the need for underlayer/photo-resist customization and optimization. [11] It is, however, becoming very clear that to meet the resolution, roughness, sensitivity, defectivity, as well as etch requirements needed for high-NA a suitable combination of resist and underlayer must be employed.

Irresistible Materials have developed the multi trigger resist (MTR) material to address the on-going requirements of EUV lithography. The MTR material is a molecular resist, which utilises ring-opening polymerisation (ROP) and incorporates a unique self-quenching mechanism, known as the multi-trigger mechanism, directly in the chemical pathways, to improve performance. The intrinsic self-quenching mechanism in the MTR material, which has been described before [12–18] provides an advantage in acid diffusion mitigation and offers a benefit on achieving ultimate resolutions with low edge roughness. After the development of the initial prototype of the resist, MTR Generation 1 (Gen1) was developed, incorporating non-metal organic high-opacity moieties for high photo-absorption. Measurements at the CXRO indicate that, depending on the level of functionalisation with the high-opacities moieties, Gen1 has an EUV absorbance of between 12.6 and 18.2 μm^{-1}. Synthesis of even more highly functionalised molecules has been achieved, and projecting from the CXRO measurements, it can be calculated that absorbances of 20–25 μm^{-1} could be achieved if required. MTR Gen1 is additionally a high-carbon content material with a low Ohnishi number, and shows low post development film thickness loss (~10%). Transfer of lines and pillar patterns from MTR films using SiN as a hard mask and standard etch processes, even from thin films (26 nm post-coat; 24 nm post-development) has been demonstrated. [19]

MTR Generation 2 (Gen2) was introduced last year. and initial results were presented. [16] In particular, we showed that good lithographic performance for P28 L/S with doses below 20 mJ/cm^2 and P36 and P34 hexagonal pillars with doses below 30 mJ/cm^2. [19,20] More recently we have explored three separate routes to significantly improve the Z-factor of the MTR system, either by increasing the activation rate of the monomer activation (Gen2.1); adjusting the relative reaction rates of the initiation and propagation rates of the ROP (Gen2.2); and via a more efficient multi-trigger quenching mechanism (Gen2.3). Here we present more detailed information on the Gen2.1 approach, together with initial results for Gen2.3, and first indications that the advantages gained by each approach are not correlated, and thus can be combined for further improvements of the MTR Z-factor (Gen2.5).

2. EXPERIMENTAL

The resist samples were prepared by dissolving the individual components in ethyl lactate or PGMEA. The solutions were then combined in various weight ratios and concentrations to give a range of formulations. The solutions undergo metal ion removal using 3M Zeta Plus filtration disks to reduce metals to levels appropriate for fab based processing.

The resist was spun onto a commercial organic underlayer, Brewer Scientific Optistack AL412, unless stated. After spin-coating of the resist the samples received a post application bake (PAB) of 80 °C for 1 minute, using a track for film deposition, and the samples were exposed to EUV using an ASML NXE3400 scanner at imec. After exposure the samples received a post exposure bake of between 60 °C and 70 °C unless stated and were developed in n-butyl acetate for 30 seconds using a dynamic system with no subsequent rinse. The patterning was observed using a Hitatchi CD-SEM (model 5000 or 6300) and the LWR, LER, LCDU and CER values are biased values as measured inline unless otherwise stated.

The baseline for the optimization is the previously introduced xMT resist system [12-18], from which the MTR Gen 1 series resist was developed. The molecular resin has been modified, to increase glass transition temperature (T_g) and to

optimize the activation energy of the MTM molecule. A cross-linking molecule which incorporates non-metal high-Z elements compared to the baseline xMT crosslinker, was introduced in the system for increased optical density in MTR Gen1. The photoacid generator was replaced in MTR Gen2.1 to optimize the ROP activation rate. Figure 1 depicts the evolution of the MTR generations. Triphenylsulfonium tosylate, which acts as a photo-decomposable quencher in epoxy-based systems, is also added [21]. Variants of MTR Gen2.1 were obtained by modifying the component ratios.

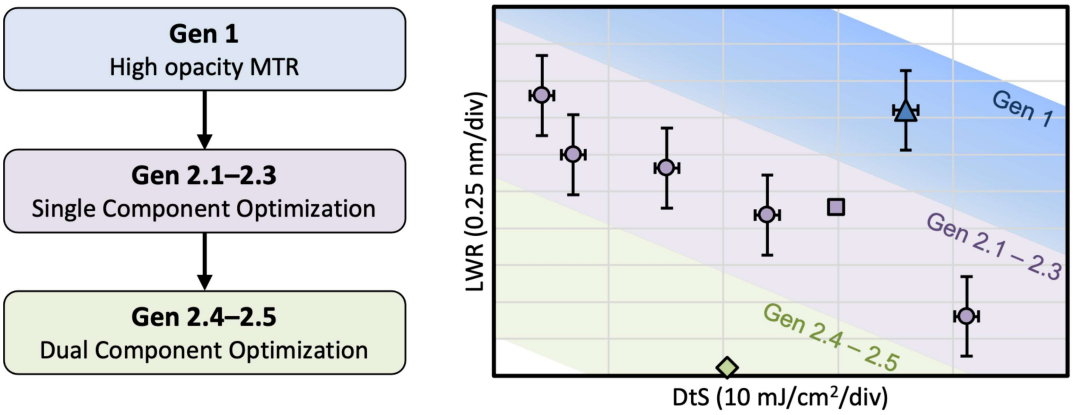

Fig 1: Schematic depicting the MTR evolution (left), together with indicative patterning performance (right). (Triangle - MTR Gen1; Circle - MTR Gen2.1; Square - MTR Gen2.3; Diamond - MTR Gen 2.5). All data collected at p28 on the NXE3400, except MTR Gen 2.3 (square) and MTR Gen2.5 (diamond), which are normalised from PSI p28 data.

3. RESULTS

3.1 Optimisation of MTR Gen2.1 for p28 lines and spaces and p34 & p36 pillars

The sensitivity improvement in seen moving from MTR Gen1 to MTR Gen2.1 resist is significant and, without a negative impact on the roughness or resolution. Figure 2 shows the LWR as a function of dose-to-size of several formulations of MTR Gen2.1 compared to MTR Gen1. It can be seen that the effect is more marked for p28 line and space (L/S) patterning (Fig. 2 (a)), than for p36 pillars (Fig. 2 (b)). As noted previously by varying the relative ratios of the MTR Gen2.1 components it is possible to optimize for either lower roughness or for higher sensitivity, depending on the application requirements.

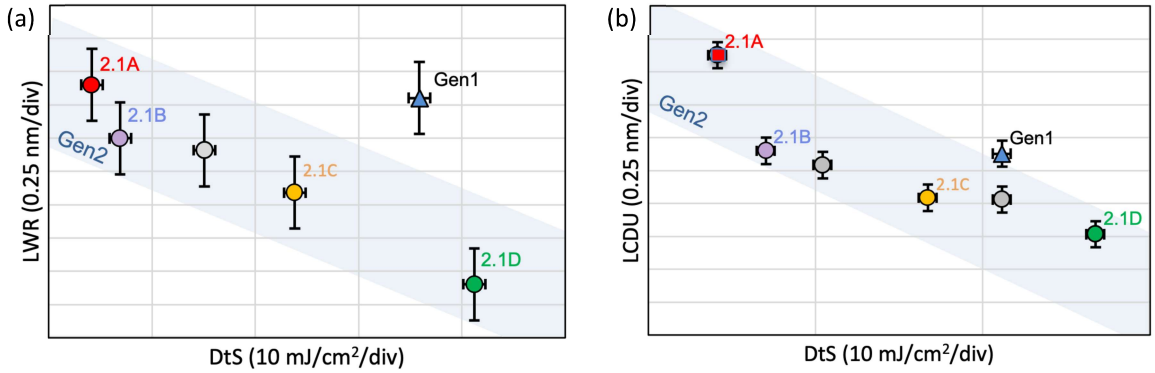

Fig 2: Comparison in dose range and roughness between MTR Gen1 and MTR Gen2.1. (a) LWR as a function of dose to size for MTR Gen2.1 variants (compared to MTR Gen1) for p28 lines and spaces; (b) LCDU as a function of dose to size for MTR Gen2.1 variants (compared to MTR Gen1) for p36 hex pillars. All exposures undertaken on the NXE3400, and with otherwise identical patterning and processing conditions.

Representative images of P28 L/S and P36 pillars obtained using the fastest formulation of the Gen 2.1 MTR series are shown in Figure 3. The film thickness for L/S was 20 nm and for pillars the resist was 21.5 nm. The dose for L/S was 19 mJ/cm^2 and for pillars 29 mJ/cm^2.

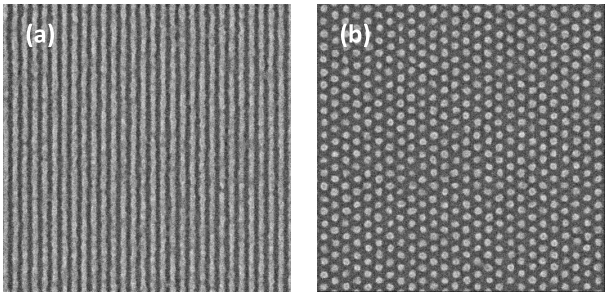

Fig 3: p28 L/S and p36 hexagonal pillars patterning in MTR Gen 2.1A; (a) Lines: CD 13.1 nm, dose 19 mJ/cm^2; (b) Pillars: CD 18.9 nm, dose 29 mJ/cm^2. Exposed using the NXE3400.

Whilst the MTR Gen2.1A can clearly resolve at the indicated pitches, the roughness is quite high. Due to the tunability of the MTR formulation, the roughness can be modulated relatively easily through formulation changes. MTR Gen2.1B, C, and D, have reduced sensitivity compared to MTR Gen2.1A but roughness and resolution improve. Figure 4 shows p34 hexagonal pillars patterned on the NXE3400 using MTR Gen2.1B, C, and D which have incrementally higher dose-to-size. The diameter of the pillars is 18 nm, and the doses are 35 mJ/cm^2 for MTR Gen2.1B, 55 mJ/cm^2 for MTR Gen2.1C and 76 mJ/cm^2 for Gen2.1D.

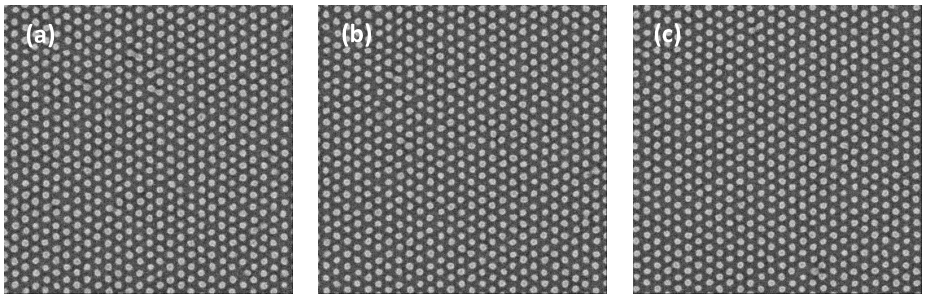

Fig 4: Hexagonal pillars of CD 18 nm patterned on the NXE3400 at p34: (a) MTR Gen2.1B, dose 35 mJ/cm^2; (b) MTR Gen2.1C, dose 55 mJ/cm^2, and (c) MTR Gen2.1D, dose 76 mJ/cm^2.

For p28 lines and spaces, the same trend is observed with roughness reducing from MTR Gen2.1B to D, with the doses used to obtain these patterns ranging from 25 to 59.5 mJ/cm^2. The CD for these p28 lines is 13.8 nm, and all exposures were performed on the NXE3400.

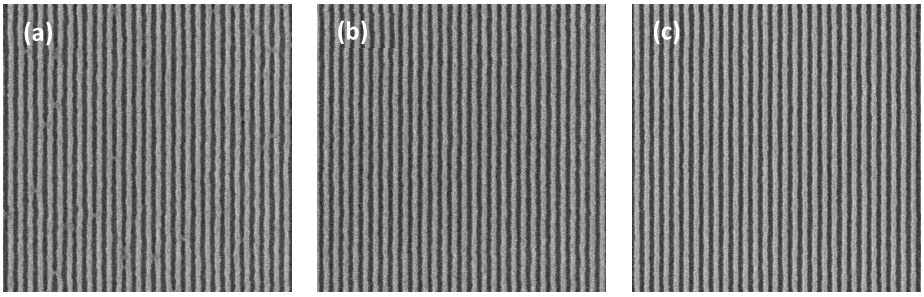

Fig 5: Lines and spaces of CD 13.8 nm patterned on the NXE3400 a p28: (a) MTR Gen2.1B, dose 25 mJ/cm^2; (b) MTR Gen2.1C, dose 42.5 mJ/cm^2; and (c) MTR Gen2.1D, dose 59.5 mJ/cm^2.

As anticipated the roughness of the lines goes down from Gen 2.1B to Gen 2.1D and the uniformity of the pillars improves, as shown in Figure 6.

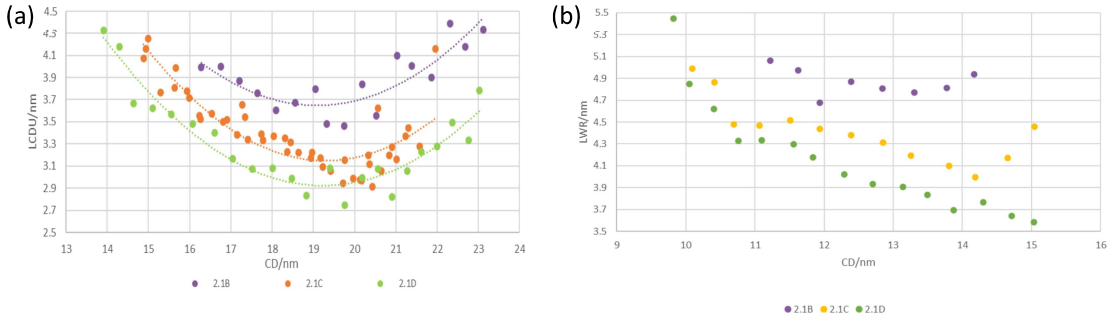

Fig 6: (a) LCDU as a function of CD in p34 pillars, and (b) LWR as a function of CD in MTR Gen2.1B, MTR Gen 2.1C, and MTR Gen2.1D.

3.2 Underlayer optimisation

The MTR material is not generally compatible with spin-on-glass (SOG) underlayers, and whilst performance can be improved with customised SOG processing, the organic Brewer Scientific OptistackAL412 underlayer [19] was found to give the best performance of a commercial underlayer. The search for the optimum underlayer, which provides good compatibility with the MTR resist and renders equal or better lithographic performance to AL412 continues. Alongside matching surface energy and chemistry of the underlayer, initial experimental data indicates that absorption might be equally important, matching the predictions of some simulation. [8]

We present here a short study on the impact the absorption of the underlayer has on the LWR, and dose-to-size of a single formulation of the MTR Gen1. Experimental underlayers were prepared by thermally curing the crosslinker component of the xMT, Gen1, and a high-opacity variant of the resist, with all other resist components removed. As the difference between the 3 underlayers was solely in the level of non-metal high-Z moity added, the surface chemistry of the 3 underlayers should be similar and well-matched to the MTR Gen1. Using the CXRO method, [22] the absorbance of the 3 underlayers is estimated as 6–8 μm^{-1}, 13–15 μm^{-1}, and 16–18 μm^{-1} for the low, medium and high absorbance respectively. Initial results show that the minimum LWR is achieved when using the medium absorbance underlayer which has a similar absorbance to the MTR Gen1 resist, whilst the high-absorbance underlayer confers a significant dose advantage, as shown in Figure 7, with the dose and LWR shown in Table 1.

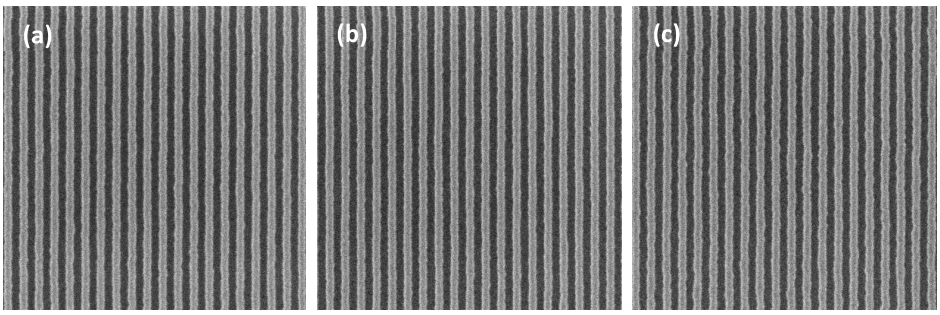

Fig 7: MTR Gen 1 patterned at p42 using an NXE3400 on experimental underlayers with (a) low (6–8 μm^{-1}), (b) medium (13–15 μm^{-1}), and (c) high (16–18 μm^{-1}), calculated absorbance. The measured absorbance of MTR Gen1 is similar to the medium absorbance underlayer.

Table 1: The effect of Underlayer absorbance on the dose and LWR of MTR Gen1.

	UL abs. < Resist abs.	**UL abs. ≈ Resist abs.**	**UL abs. > Resist abs.**
Dose (mJ/cm^2)	75.5	72.5	60.5
LWR (nm)	2.31	2.22	2.91

4.CONCLUSIONS

The lithographic performance of several MTR Gen2.1 formulations was shown. The fastest variant of MTR Gen2.1 was shown to have a sensitivity 3 times higher than the Gen 1 MTR material, with only a very small increase in LWR in L/S patterning, whilst the sensitivity could be doubled for hexagonal pillar patterning whilst maintaining LCDU. MTR Gen2.1 optimizes the monomer activation rate, and similar performance enhancements are seen by optimizing the initiation and propagation reaction rates (MTR Gen2.2 [20]), and improving the multi-trigger efficiency (MTR Gen2.3; initial PSI data presented here, figure 1). Further these performance gains appear to be non-correlated and the gains of MTR Gen2.1 and MTR Gen2.3 can be combined to achieve further improvements (MTR Gen2.5; initial PSI data presented here, figure 1).

ACKNOWLEDGEMENTS

The authors would like to thank the Engineering and Physical Sciences Research Council (EPSRC) for support of this project. The authors thank Irresistible Materials Ltd. and Nano-C for support and provision of resist materials. The authors thank Terry Mcafee, Oleg Kostko, Patrick Naulleau, and James Blackwell for absorbance measurements at CXRO.

REFERENCES

[1] Nagahara, S., Que Dinh, C., Yoshida, K., Shiraishi, G., Kondo, Y., Yoshihara, K., Nafus, K., Petersen, J.S., De Simone, D., Foubert, P., Vandenberghe, G., Stock, H-J, Meliorisz, B., "EUV resist chemical gradient enhancement by UV flood exposure for improvement in EUV resist resolution, process control, roughness, sensitivity, and stochastic defectivity," *Proc. SPIE*, **11326**, 113260A (2020).

[2] Shirotori, A., Hoshino, M., De Simone, D., Vandenberghe, G., Matsumoto, H., "A novel main chain scission type photoresists for EUV lithography", *Proc SPIE*, **11517**, 115170D (2020).

[3] Sharma, S.K., Kumar, R., Chauhan, M., Moinuddin, M.G., Peter, J., Ghosh, S., Pradeep, C.P., Gonsalves, K.E., "All-new nickel-based Metal Core Organic Cluster (MCOC) resist for N7+ node patterning," *Proc SPIE*, **11326**, 1132604 (2020).

[4] Torok, J., Del Re, R., Herbol, H., Das, S., Bocharova, I., Paolucci, A., Ocola, L. E., Ventrice Jr., C., Lifshin E., Denbeaux, G., Brainard, R. L., "Secondary Electrons in EUV Lithography," *J Photopolym. Sci. Technol.*, **26**, 625–634 (2013).

[5] Thackeray, J., Cameron, J., Jain, V., LaBeaume, P., Coley S., Ongayi O., Wagner M., Rachford A., Biafore J., "Progress in Resolution, Sensitivity and Critical Dimensional Uniformity of EUV Chemically amplified Resists," *Proc. SPIE*, **8682**, 868213 (2013).

[6] Nakano, A., Kozawa, T., Okamoto, K., Tagawa, S., Kai, T., Shimokawa, T., "Acid Generation Mechanism of Poly(4-hydroxystyrene)-Based Chemically Amplified Resists for Post-Optical Lithography: Acid Yield and Deprotonation Behavior of Poly(4-hydroxystyrene) and Poly(4-methoxystyrene)," *Jpn. J. App. Phys.,* **45**, 6866–6871 (2006).

[7] Narasimhan, A., Wisehart, L., Grzeskowiak, S., Ocola, L.E., Denbeaux, G., Brainard, R. L., "What we don't know about EUV exposure mechanisms," J Photopolym. Sci. Technol., **30**, 113–120 (2017).

[8] Long, L.T., Neureuther, A., Walraff, G., Naulleau, P. "Resist Underlayer Simulations," In *IEUVI TWG April 2022*, 7, (2022), http://ieuvi.org/TWG/Resist/IEUVI_Resist01.htm (Accessed 13/02/2023).
[9] Raley, A., Huli, L., Grzeskowiak, S., Lutker-Lee, K., Krawicz, A., Feurprier, Y., Liu, E., Kato, K., Nafus, K., Dauendorffer, A., Bae, N., LaRose, J., Metz, A., Hetzer, D., Honda, M., Nishizuka, T., Ko, A., Okada, S., Ido, Y., Onitsuka, T., Kawakami, S., Fujimoto, S., Shimura, S., Dinh, C.Q., Muramatsu, M., Biolsi, P., Mochiki, H. and Nagahara, S., "Outlook for high-NA EUV patterning: a holistic patterning approach to address upcoming challenges," *Proc SPIE*, **12056**, 120560A (2022).
[10] Severi, J., Lorusso, G.F., De Simone, D., Moussa, A., Saib, M., Duflou, R., De Gendta, S., "Chemically amplified resist CDSEM metrology exploration for high NA EUV lithography," *J Micro/Nanopattern. Mater. Metrol.*, **21**, 021207 (2022).
[11] Fallica, R., De Simone, D., Chen, S., Safdar, M. and Suh, H.S., "Scaling and readiness of underlayers for high-NA EUV lithography," *Proc* SPIE, **12292**, 122920V (2022).
[12] Vesters, Y., McClelland, A., Popescu, C., Dawson, G., Roth, J., Theis, W., de Simone, D., Vandenberghe, G., Robinson, A.P.G, "Multi-trigger resist patterning with ASML NXE3300 EUV scanner," *Proc. SPIE*, **10586**, 1058308 (2018).
[13] Popescu, C., Kazazis, D., McClelland, A., Dawson, G., Roth, J., Theis, W., Ekinci, Y., Robinson, A.P.G., "High-resolution EUV lithography using a multi-trigger resist," *Proc SPIE*, 10583, 105831L (2018).
[14] O'Callaghan, G., Popescu, C., McClelland, A., Kazazis, D., Roth, J., Theis, W., Ekinici, Y., Robinson, A.P. G., "Multi-trigger resist – Novel synthesis improvements for high resolution EUV lithography," *Proc SPIE*, **10960**, 109600C (2019).
[15] Montgomery, W., McClelland A., Ure D., Roth J., Robinson A., "Irresistible Materials multi-trigger resist: the journey towards high volume readiness," *Proc SPIE*, **10143**, 1014328 (2017).
[16] Popescu, C., McClelland, A., Kazazis, D., Dawson, G., Roth, R., Ekinci, Y., Theis, W. and Robinson, A. P.G., "Multi-trigger resist for electron beam and extreme ultraviolet lithography," *Proc SPIE*, **10775**, 1077502 (2018).
[17] Popescu C., O'Callaghan G., McClelland A., Roth J., Lada T., Robinson A.P.G., "Performance enhancements with high opacity multi-trigger resist," *Proc SPIE*, **11326**, 1132611 (2020).
[18] Popescu, C., O'Callaghan, G., McClelland, A., Roth, J., Lada, T., Kudo, T., Dammel, R., Moinpour, M., Cao, Y., Robinson, A. P. G., "Progress in the multi-trigger resist," *Proc SPIE*, **11612**, 116120K (2021).
[19] Popescu, C., O'Callaghan, G., McClelland, A., Roth, J., Jackson, E., Robinson, A. P. G., "Component optimization in the multi-trigger resist," *Proc SPIE*, **12055**, 120550G (2022).
[20] Popescu, C., O'Callaghan, G., McClelland, A., Storey, C., Roth, J., Jackson, E. and Robinson, A.P.G., " Recent accomplishments in EUV lithography patterning for multi-trigger resist," *Proc SPIE*, **12292**, 122920E (2022).
[21] Lawson, R.A., Frommhold, A., Yang, D.X., Robinson, A.P.G, "Negative-tone organic molecular resists," In *Frontiers of Nanoscience*: *Materials and Processes for Next Generation Lithography*, **Vol. 11**, Robinson A.P.G. and Lawson R.A. eds., (Oxford: Elsevier, 2016). pp. 223-317.
[22] https://henke.lbl.gov/optical_constants/atten2.html (Accessed 13/02/2023).